

The NaK Population: a 2019 Status

Mark Matney⁽¹⁾, Phillip Anz-Meador⁽²⁾, James Murray⁽²⁾, Rossina Miller⁽²⁾, Timothy Kennedy⁽¹⁾

⁽¹⁾ NASA Johnson Space Center, Mail Code XI5-9E, 2101 NASA Parkway, Houston, TX 77058, USA,
mark.matney-1@nasa.gov

⁽²⁾ Jacobs JETS Contract, NASA Johnson Space Center, Mail Code XI5-9E, Houston, TX 77058, USA

ABSTRACT

The statistical debris measurement campaigns conducted by the Haystack Ultrawideband Satellite Imaging Radar (HUSIR) on behalf of the NASA Orbital Debris Program Office are used to characterize the long-term behavior of the small, low Earth orbit (LEO) orbital debris environment. A long-recognized, unique component of the LEO environment is composed of small Sodium-Potassium (NaK) eutectic nuclear reactor coolant droplets associated with the Soviet Radar Ocean Reconnaissance Satellite (RORSAT) program. Beginning with the flight of Cosmos 1176, RORSAT vehicles would nominally separate their reactor core at end of mission, thereby venting the NaK coolant and producing the NaK droplet population.

In this paper, we describe the methodology by which NaK are segregated from the statistically sampled general debris population and their sizes inferred; the current NaK environment; how it has changed over time; and a potential new source of NaK: RORSAT vehicles that did not separate their reactor core by either design or apparent malfunction.

1 INTRODUCTION: OVERALL ENVIRONMENT HISTORY

The NaK population was originally identified in the early 1990s in Goldstone and Haystack radar data. It represented a population of electrically conducting spheres from a few millimeters in size to a few centimeters, all in 65° inclination, near-circular orbits, mostly between the altitudes of 850 km and 1000 km. The spherical nature was deduced from the polarization of the radar returns, which indicated a strong principal polarization (PP) and a very weak orthogonal polarization (OP). Further work by Lincoln Laboratories succeeded in cataloging a few of these objects, determining their ballistic coefficients, and measuring their optical properties [1, 2]. All the evidence pointed to electrically conducting spheres, with densities consistent with the sodium-potassium liquid metal coolant used in the Soviet Radar Ocean Reconnaissance SATellite (RORSAT) reactors that jettisoned their nuclear cores into these orbits in the 1980s. In the microgravity of orbit, the liquid droplets formed into individual spheres. In addition to the RORSAT source, TOPAZ reactors (aboard Cosmos 1818 and 1867) have also been noted to produce NaK droplets in their operational orbits, though they did not separate reactor cores.

2 NaK POPULATION

2.1 Brief History of NaK Sources

Operational US-A (*Upravlenkiye Sputnik-Aktivny*), or RORSAT, spacecraft were powered by the Бук reactor (Anglicized variously as Bouk or Buk, pronounced bōōk as in moon). Beginning with the test spacecraft Cosmos 198 (International Designator 1967-127A, Space Surveillance Network [SSN] catalog #3081), RORSATs effected an end-of-mission disposal orbit maneuver, placing the propulsion unit/reactor module in a high-altitude, long-lifetime disposal orbit. With the launch of Cosmos 1176 (1980-034A, SSN #11788), the reactor core was separated from the reactor module to further extend the on-orbit lifetime of the highest radioactivity fuel elements (while noting that the radioactive half-life of ²³⁵U is over 700 Ma, obviously much longer than natural decay from the disposal orbit altitude [3]).

The reactor system featured a primary and secondary coolant loop; the primary loop could vent to space upon core separation. A NaK mass of 13 kg is resident in the primary loop, of which 5.3 kg is the current estimate of mass released during core ejection [4]. The two TOPAZ reactor test flights aboard *Plazma-A* spacecraft, Cosmos 1818 and Cosmos 1867, are estimated to carry approximately 15.5 kg NaK mass [5]. Table 1 summarizes RORSAT

flights producing cataloged NaK coolant and/or separating their reactor cores over the lifecycle of the RORSAT operations, and *Plazma-A* test programs.

Table 1. Historical NaK Source Flights

MODEL NaK Dispersal Number	Parent International Designator	SSN Catalog Number Parent:Core	Common Name	MODEL Separation Date YYYY:DDD	Orbit Type	Apogee Alt. [km]	Perigee Alt. [km]	Inclination [deg]	Comments: (n) indicates n cataloged COOLANT objects, 5 August 2019 epoch
N/A	1976-103A	9486	COSMOS 860	N/A	3	967	901	64.7	(3)
1	1980-034A	11788:11971	COSMOS 1176	1980:254	1	970	873	64.8	first core separation; (2)
2	1981-021A	12319:12551	COSMOS 1249	1981:169	1	990	898	65.0	(17)
3	1981-037A	12409:12435	COSMOS 1266	1981:118	1	969	893	64.8	(1)
4	1981-081A	12783:12808	COSMOS 1299	1981:242	1	985	911	65.1	
5	1982-043A	13175:13594	COSMOS 1365	1982:269	1	982	886	65.1	
6	1982-052A	13243:13416	COSMOS 1372	1982:222	1	982	909	64.9	
N/A	1982-084A	13441:13748	COSMOS 1402	N/A	4	250	240	65.0	apparent disposal orbit insertion failure
7	1982-099A	13600:13653	COSMOS 1412	1982:314	1	984	908	64.8	(1)
8	1984-069A	15085:15330	COSMOS 1579	1984:270	1	988	904	95.1	(31)
9	1984-112A	15378:15503	COSMOS 1607	1985:032	1	997	911	65.0	
10	1985-064A	15930	COSMOS 1670	1985:295	1	990	898	64.7	core not cataloged/identified
11	1985-075A	15986	COSMOS 1677	1985:296	1	990	918	64.9	core not cataloged/identified
12	1986-024A	16647:16809	COSMOS 1736	1986:172	1	1013	925	65.0	
13	1986-062A	16917:17035	COSMOS 1771	1986:288	1	999	917	65.0	
N/A	1987-011A	17369	COSMOS 1818	N/A	2	800	775	65.0	Plazma-A/TOPAZ; (29)
14	1987-052A	18122:18241	COSMOS 1860	1987:209	1	992	907	65.0	
N/A	1987-060A	18187	COSMOS 1867	N/A	2	800	775	65.0	Plazma-A/TOPAZ; (40)
15	1987-101A	18665	COSMOS 1900	1988:274	1	763	695	66.1	core not cataloged/identified
16	1988-019A	18957:19162	COSMOS 1932	1988:140	1	1012	924	65.0	

Notes: orbit types are RORSAT disposal orbit (1); *Plazma-A* operational orbit (2); RORSAT disposal orbit without core separation (3); and RORSAT operational orbit (4). Historical RORSATs prior to Cosmos 1176 omitted without production of catalogued COOLANT objects. Model parameters after Xu, *et al.* [6].

Table 1's adjective "MODEL" indicates the event and core disposal orbit used in certain NASA Orbital Debris Program Office (ODPO) modeling activities. Tabulated flights without a MODEL NaK dispersal number are not modeled explicitly as a dispersal event. This paper's section 3.3 discusses efforts to implement a NaK model in the current engineering model development.

2.2 New Sources

Difficulties were encountered when attempting to match modelled NaK particle clouds from dispersal events with radar observations. In particular, it has been noted that small particles are resident at altitudes that should have been cleared of NaK droplets if the droplets had indeed been deposited in single events in the past. This suggests an ongoing release of small NaK droplets between 900 km and 1000 km altitudes. Possible sources include post-Cosmos 1176 RORSATs venting additional mass from their primary coolant loops; post-Cosmos 1176 RORSATs whose cores did not separate nominally; and RORSATs whose secondary coolant loops have leaked due to micrometeoroid/orbital debris (MMOD) impact or structural fatigue/failure, perhaps due to thermal cycling.

In the case of the first hypothesis, any post-Cosmos 1176 could presumably vent additional mass from their open primary coolant loop, perhaps dependent upon lighting and thermal conditions and experiencing regular "seasons" of small particle release events. Cosmos 1670 and 1677 are candidates for the second hypothesis, as the SSN public catalogue does not include the cores; the Cosmos 1900 core is also not catalogued, but its lower altitude removes it from consideration as a source. Finally, all RORSATs in Table 1, in addition to Cosmos 367 (generally believed to be the first launch of a live reactor [7]); 402, 469, 516, 626 (generally believed to be the first nominal RORSAT mission); 651, 654, 723, 724, 785, 861, and 952, could potentially contribute to the environment in events described in hypothesis three. Analysis and modeling are ongoing in an effort to better understand the production of NaK droplets.

3 Measuring and Modeling the NaK Population

3.1 NaK Identification

The NaK population was originally identified near 65° inclination and mostly between altitudes of 850 km and 1000 km, forming individual, electrically conducting spheres in the microgravity environment. Using this background, a filter may be developed for extracting the NaK population from the rest of the orbital debris environment. A plot of orbital debris detected by the Haystack Ultra-wideband Satellite Imaging Radar (HUSIR) over the years 2014–2017 in altitude and Doppler inclination is shown in Fig. 1, with the debris cloud that includes the NaK population highlighted. To better diagram members of the debris cloud, an initial filter in Doppler inclination, $62.9^\circ < \text{Doppler inclination} < 67^\circ$, and altitude < 1000 km is used to separate this debris cloud from the rest of the orbital debris environment.

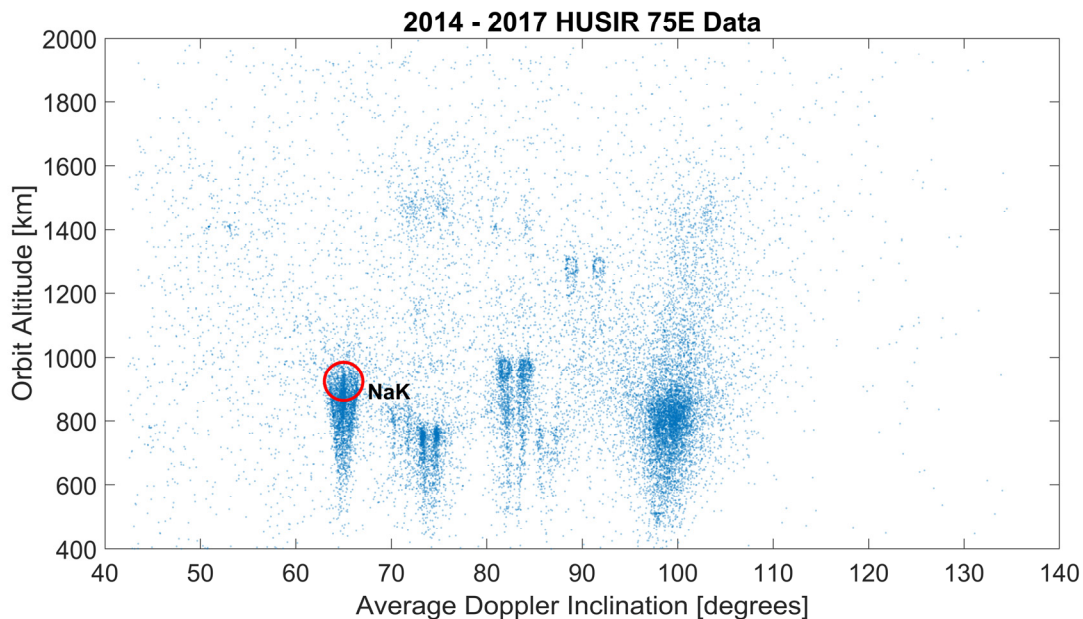


Fig. 1. HUSIR orbital debris observations for 2014–2017 in altitude and Doppler inclination space. The orbital debris cloud containing the NaK population is highlighted. Regions with predominately circular or near-circular orbits appear as vertical stripes in the data, and clearly are grouped into clumps that correspond to orbit regions where many satellites are concentrated. The geometry of northward-moving and southward-moving orbiting objects viewed with the 75° east-pointing geometry creates the “twinning” effect visible for each grouping of objects. The true inclination of these bands is halfway between the “twin” stripes.

Since the NaK droplets are spherical and electrically conductive, the reflection of an incident, circularly polarized wave is also circularly polarized; however, the reflected energy reverses polarization handedness, *i.e.*, a right-hand incident wave produces a left-hand – principal polarization (PP) component – backscattered wave. The backscattered, right-hand, circularly polarized, orthogonal-polarization (OP) component is ideally zero for the perfectly conducting sphere. Differences arise if the droplets are not perfectly spherical and at smaller signal-to-noise ratios (SNR) – equivalently smaller sizes – where noise power in the sensor measuring the OP component is such that the polarization appears to be a mix of both right- and left-hand polarizations. A polarization filter is developed to separate the cluster of highly PP polarized objects from the rest of the objects detected in the altitude and inclination region where the NaK particles reside. This is shown in Fig. 2, where the piecewise linear decision boundary – the dashed black line – is constructed by inspection.

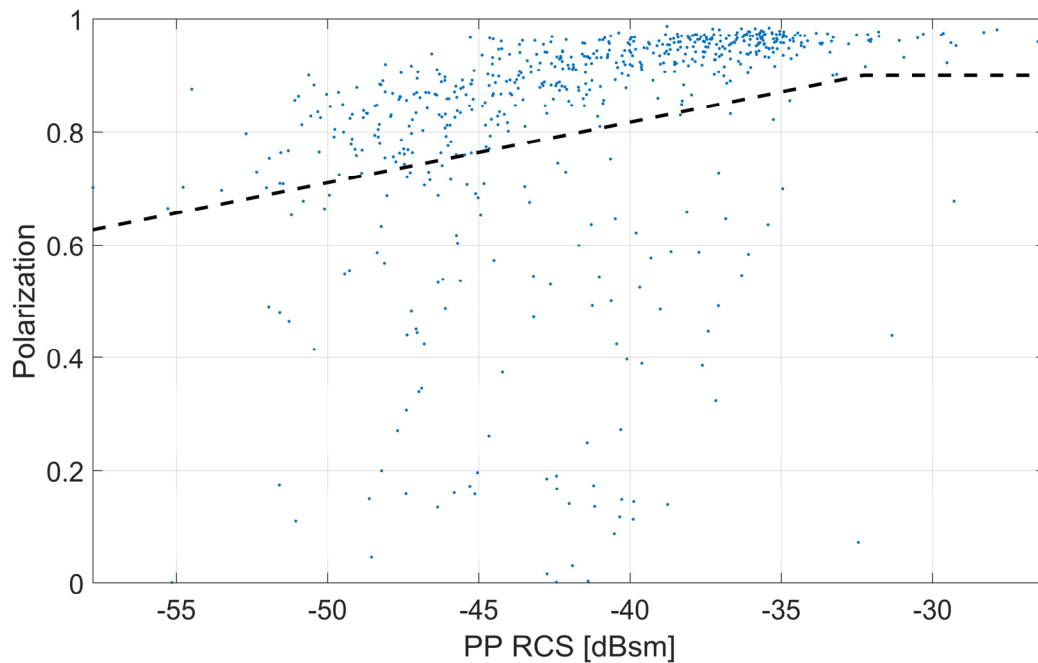


Fig. 2. Orbital debris observations in polarization and RCS space (polarization > 0 shown), after filtering on altitude < 1000 km and $62.9^\circ < \text{Doppler inclination} < 67^\circ$ for radar observations from calendar year 2014. Polarization is defined as $[(PP-OP)/(PP+OP)]$, such that a high-PP object should have polarization near +1.0. A piecewise linear boundary – the dashed black line – separates the NaK (above the boundary) from the rest of the orbital debris population in this altitude and Doppler inclination region.

Clustering approaches also may be useful to pick out this structure, such as application of a Gaussian mixture model to the objects shown in Fig. 3. The contour lines shown in this figure represent the likelihood (the likelihood scale is shown on the right side of the figure) that an orbital debris object belongs to the cluster of orbital debris associated with the NaK population. The decision boundary obtained by inspection to separate the NaK population in polarization and RCS space is in good agreement with the approach using the Gaussian mixture model.

Note that any method applied will not be perfect. There may still be non-NaK debris masquerading as NaK debris, and NaK that the screening process misses. However, the techniques presented should minimize the percentage of non-NaK debris and maximize the number of true NaK debris in the population for our studies.

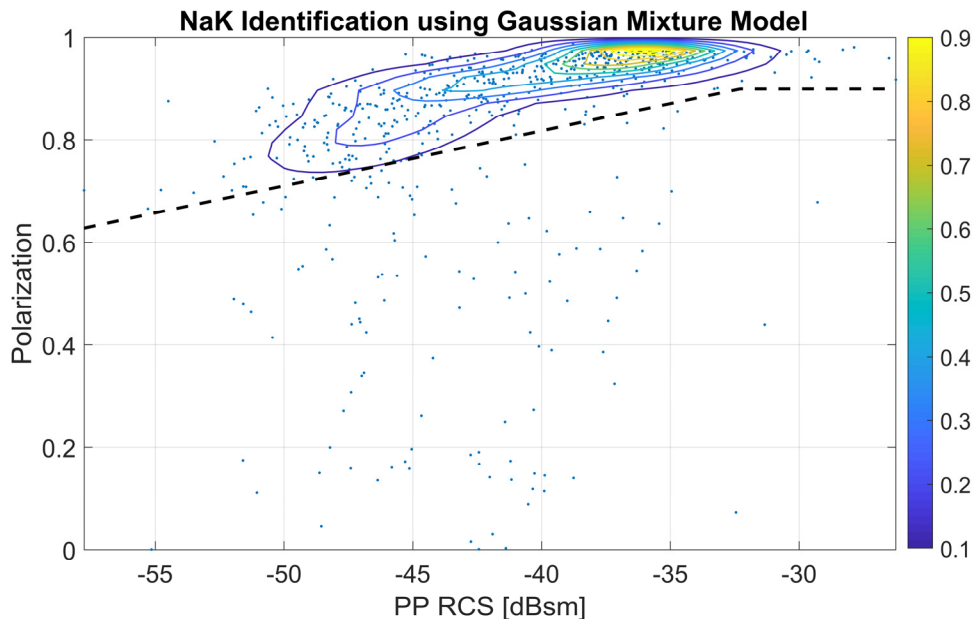


Fig. 3. Identification of the NaK population through clustering, using a Gaussian Mixture Model. Note that there is good agreement between the piecewise-linear and clustering-based approach.

3.2 Usage of NaKs as Calibration Spheres

The NaK cumulative count rates, after extracting the NaK droplets from the rest of the orbital debris population, as a function of RCS are shown in Fig. 4, along with Poisson sampling error 2σ uncertainties. Uncertainties are indicated by the shaded areas of the same color as the respective count rate for a given calendar year. The cumulative count rates for the NaK population are stable for the years considered here, and in general are statistically equivalent to each other. It should be noted that differences at the smaller RCS, for example in 2017 where the transmitter power was significantly reduced due to multiple amplifier failures, may be due, in large part, to a change in sensitivity for HUSIR in a given year.

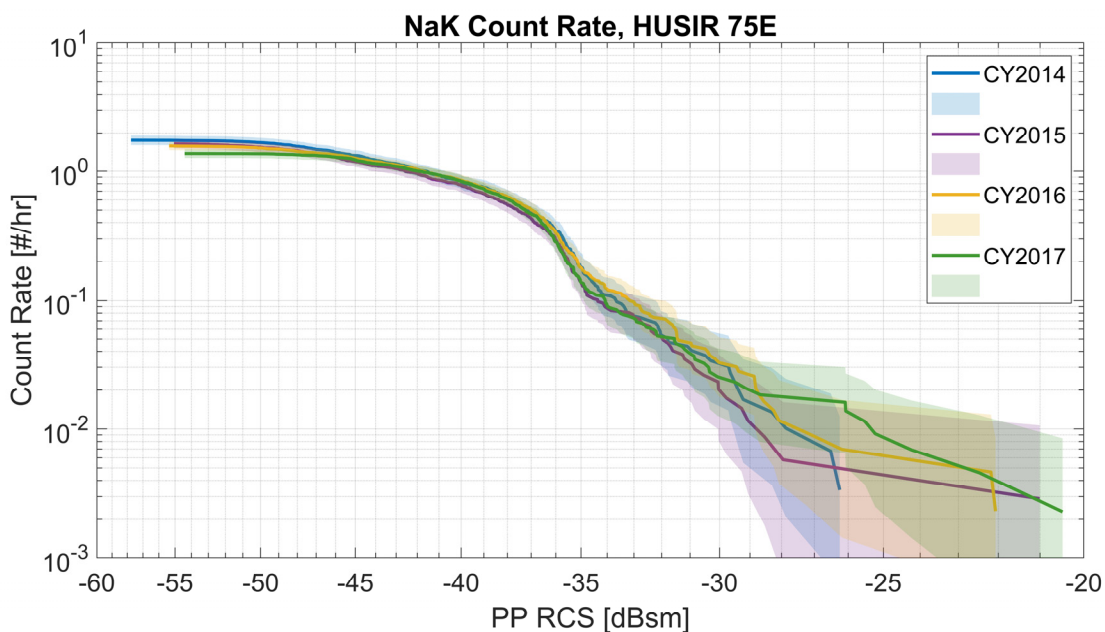


Fig. 4. Cumulative count rate for the NaK population with 2σ Poisson uncertainties.

The shape of the cumulative-count-rate curve is related to the unique properties of the NaK population. As it turns out, the NaK droplets are an excellent calibration source. For the HUSIR radar wavelength, it is expected that the NaK population will have a “spike” in the count rate for particles with an RCS near -35 dBsm. This increased count rate is due to the distribution of the radar cross section of the NaK particles in the Mie resonance region. The RCS for the case of Mie scattering for a sphere as a function of size (diameter) at the HUSIR wavelength is shown in Fig. 5, where a horizontal line marks the inflection point where the -35 dBsm is indicated. A cumulative, empirical NaK model for observations at the HUSIR wavelength is shown in Fig. 6 as a function of RCS [8, 9], where a similar -35 dBsm vertical line is also plotted. The sudden increase in cumulative counts for the model near the reference RCS line is visible in the data, as shown in Fig. 4, where an increased count rate at this RCS (-35 dBsm) is evident.

This behaviour is solely a function of the wavelength of a radar interacting with conducting spheres. It should be independent of the radar and the individual sizes of the NaK particles detected. The NaK population is believed to consist of a continuum of sphere sizes due to the random nature of the droplet production. Therefore, as long as there are sufficient NaK detections with sizes that return RCS values around -35 dBsm, or whatever this critical RCS value is for a given radar’s wavelength, this feature should be present to aid in radar calibration studies. Deviances in the location or shape of this feature would indicate periods where the sensor is not properly calibrated.

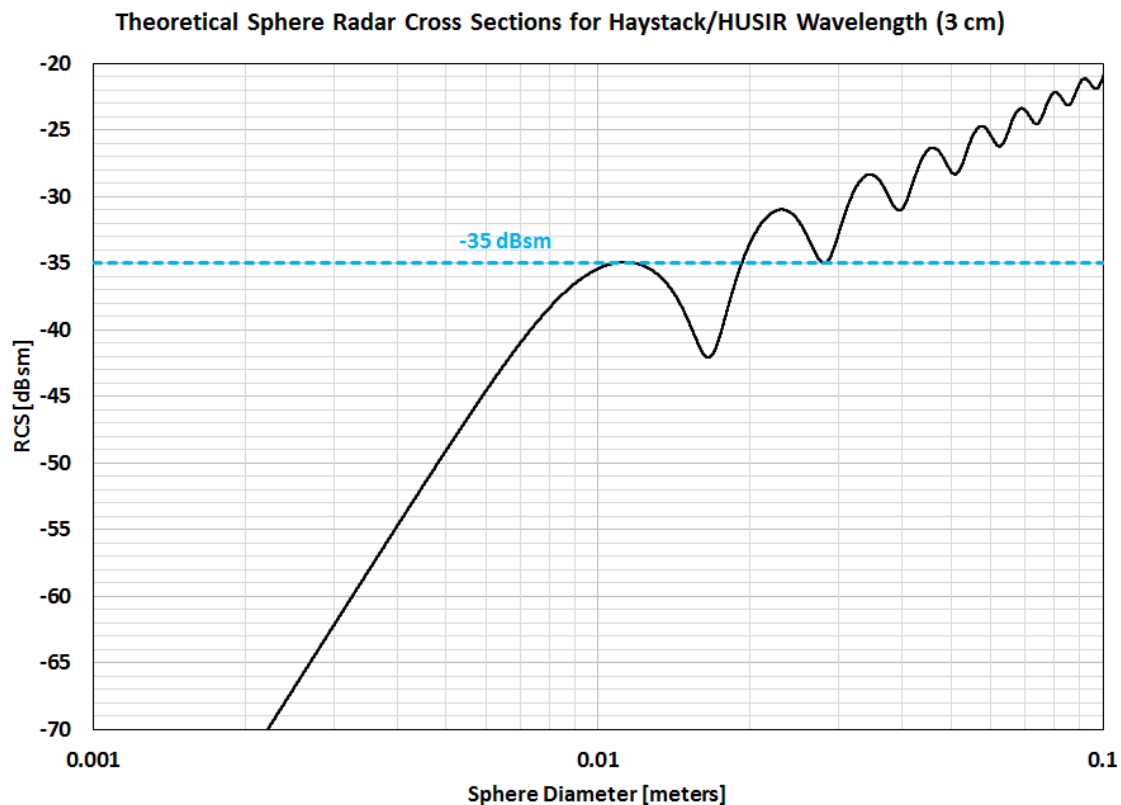


Fig. 5. Mie scattering for spheres at the HUSIR X-band wavelength. A reference line at -35 dBsm is shown, which marks the primary inflection of the RCS curve where a sudden change in the cumulative count rate for NaK is expected at the HUSIR wavelength.

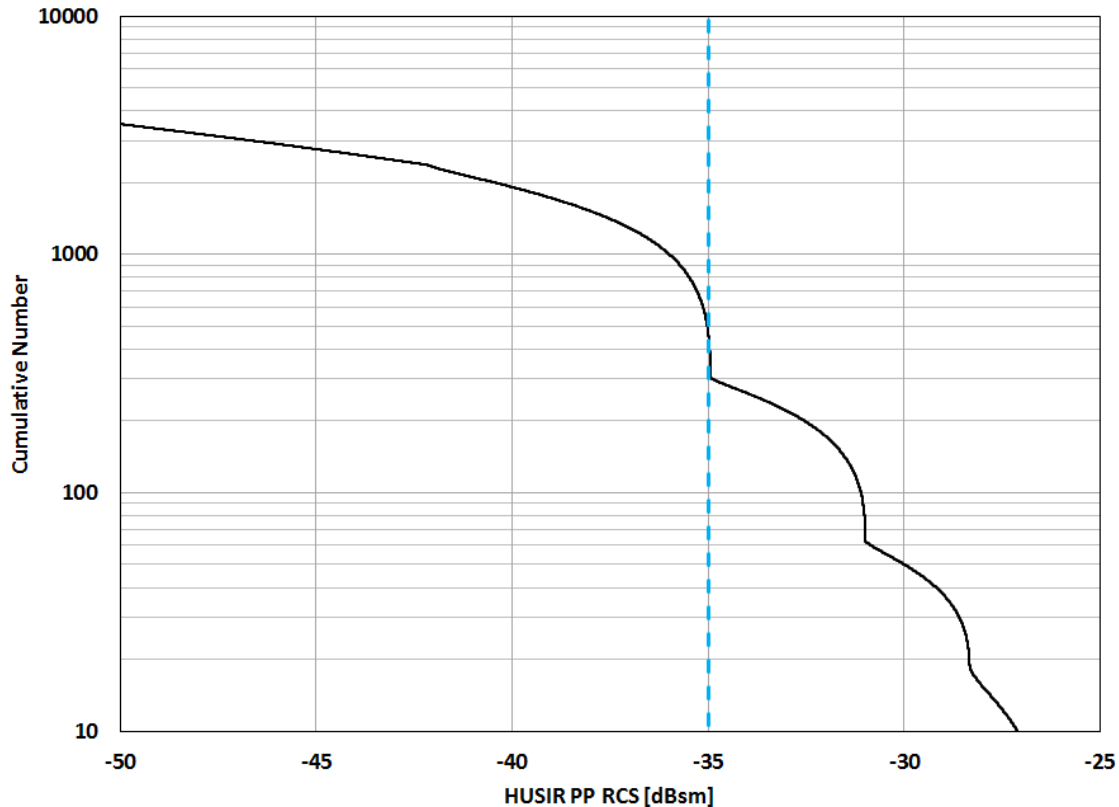


Fig. 6. Model for the cumulative count of the on-orbit NaK population as a function of RCS at the HUSIR wavelength. The primary feature at -35 dBsm is marked by the dashed blue line. The empirical size distribution is based on the work of Foster [8, 9]

3.3 Population Used in ORDEM 3.1

Over the years, the NASA ODPO has developed a series of Orbital Debris Engineering Models (ORDEM). The ORDEM software currently serves as the primary tool to provide a timely, validated model of the human-made orbital debris environment. It facilitates modeling assessments by spacecraft owner/operators and for ground-based observation planning. The debris populations in ORDEM are divided into different material density classes, which are modeled separately. The NaK population, due to its unique density $\sim 0.9 \text{ g/cm}^3$, is modeled as a separate population.

The orbital debris environment is dynamic and must be updated periodically. As newer datasets become available, they provide more information on the evolution of the orbital debris environment. In addition, newly developed data analysis techniques can be applied to both new and legacy data to improve the assessment of orbital debris populations. The newest version of ORDEM is known as ORDEM 3.1, and it incorporates the newest and highest fidelity datasets available to NASA for both constructing and validating the modeled orbital debris populations. ORDEM 3.1 is in the final stages of development and review and represents NASA's best estimate of the current and near future orbital debris environment.

Modeling for previous ORDEM models had assumed that the deposition of the NaK took place only at the times the RORSAT cores were jettisoned (Table 1). The newest HUSIR data encompasses another solar cycle from the radar data used in the previous ORDEM model, and gives an indication how the droplet orbits have decayed over the latest solar cycle maximum. As seen in Fig. 7, the 2014 HUSIR data shows a significant contribution of small (less than $\sim 6 \text{ mm}$) droplets at the highest altitudes, where atmospheric drag should have removed them by now. This indicates that there is some sort of continual source for these small droplets at higher altitudes, as discussed in Section 2.2. Likely, these reservoirs are RORSATs that did not jettison reactor cores or possibly segments of the RORSAT satellites that still have residual NaK coolant in their pipes. Additionally, the recent anomalous debris

events linked to the TOPAZ reactor spacecraft may correspond to ongoing sporadic leakage events. Because of these apparent continual sources, for ORDEM 3.1, the NaK population was modeled as a steady state over the future projections of the model. Until further analysis reveals the causes and details of ongoing production events, this is a reasonable conjecture.

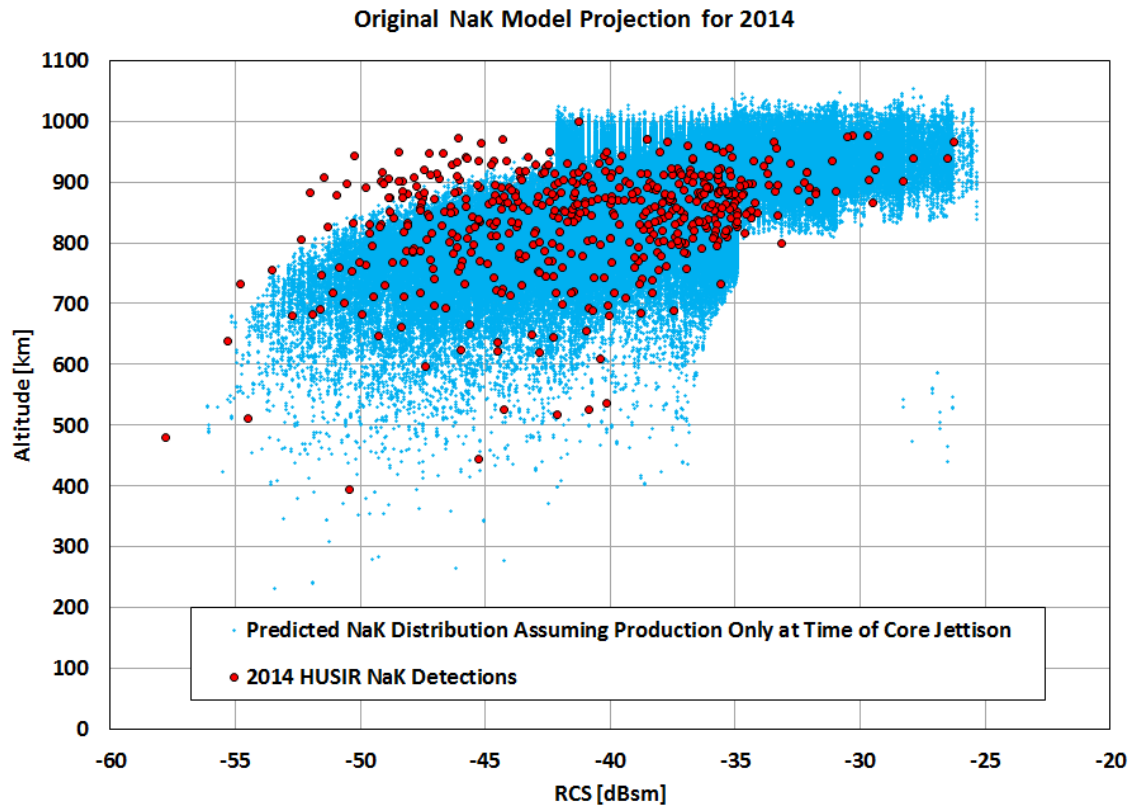


Fig. 7. NaK Distribution in RCS predicted by assuming production only at time of RORSAT core jettison (blue), compared to the NaK detections from the 2014 HUSIR 75°E data (red). While in general, low RCS corresponds to smaller size, the relationship between size and RCS for conducting spheres is complicated (see Fig. 5). For HUSIR, objects with RCS values smaller than -43 dBsm correspond to NaK spheres with diameters smaller than 6.42 mm. Note how the model predicts that NaK with small RCS should have decayed down to lower altitudes, while the radar data still shows a substantial population of small RCS NaK spheres at higher altitudes that resembles the altitude distribution of larger NaK spheres.

To construct a steady-state ORDEM population, all that is needed is a reference NaK model for a given date, which is then simply replicated for all years. The easiest approximation is to model the NaK population as a single inclination (65°) and single eccentricity (circular orbits), and use an empirical distribution in altitude and size.

Ascertaining the sizes of individual NaK particles is complicated by the fact that, as spheres, certain RCS values can correspond to up to three different sizes. This means that for certain RCS values, the size determination can be ambiguous. Fortunately, the HUSIR data observes objects well into the Rayleigh regime of the size-RCS curve, where the object size is much smaller than the radar wavelength, and where the RCS-to-size conversion is less ambiguous.

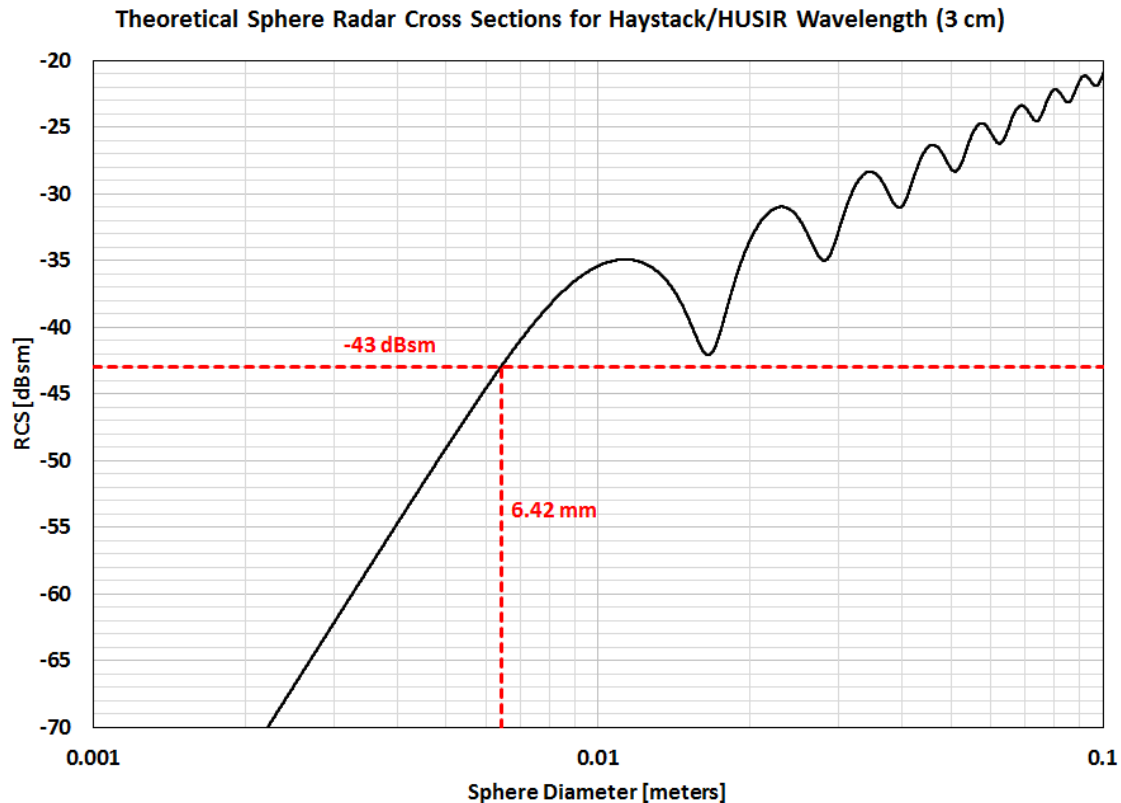


Fig. 8. The black curve shows the RCS value for a given conducting sphere diameter (given the Haystack/HUSIR 3 cm wavelength). The red dashed line is for an RCS of -43 dBsm, corresponding to a sphere 6.42 mm in diameter. For Haystack/HUSIR detections of objects with RCS values above about -43 dBsm, there is an ambiguity in determining the size of the object, but objects with RCS below that value have a much simpler relationship of RCS to size. Therefore, counting the number of detections with RCS above -43 dBsm gives an unambiguous estimate of the total number of spheres larger than 6.42 mm in diameter.

Choosing NaK particles (filtered out of HUSIR data that provided a high PP/OP ratio, altitudes below 1000 km, and inclinations near 65°) with RCS smaller than -43 dBsm square meters provides a representative accurate count of all NaK particles detected larger than approximately 6.42 mm. Previous work [8, 9] estimated the overall size distribution of the NaK population by fitting a functional form to the size curve and predicting the corresponding RCS distribution. The size distribution was varied until the computed RCS curve matched the data. This size distribution, used to scale the 6.42 mm populations to the ORDEM reference sizes, is presented in Table 2.

Each NaK object seen represents some number of unseen NaK objects. For a given radar pointing configuration (*e.g.*, 75° elevation pointing east, which is the standard observation mode for HUSIR), an object in a circular orbit and known inclination will have a certain detection rate. By comparing the number of detected objects in that orbit to the number expected, it is possible to scale the size of the unseen component of the population. The expected detection rate of a particular detected NaK object is first determined from the radar geometry, using the knowledge that the NaK particles are in nearly circular orbits at 65° inclination, and with altitude given by the altitude of detection. The probability of seeing a single object in such an orbit was computed by multiplying the detection rate by the total observation time. Each object seen was then weighted by the inverse of its detection probability, and the resulting sum over all NaK objects detected in a particular altitude bin provided a statistical estimate of the NaK population in that bin.

Table 2. The multiplicative factors used to scale the unambiguous count at 6.42 mm size to the ORDEM fiducial sizes

NaK Sphere Reference Size	Model Ratio of Empirical NaK Population Fit to Measured 6.42 mm NaK Population
3.16 cm	0.0244
1.0 cm	0.532
3.16 mm	2.30
1.0 mm	8.25

4 CONCLUSIONS

The NaK population presents both a unique challenge and a unique opportunity to modeling and measuring the orbital debris environment. The distinctive behavior of a distribution of different size-conducting spheres allows us to extract the NaK particles with high confidence from the rest of the debris population, and to use their distributions in RCS to provide a secondary calibration to the radar data. Because we have now observed this population over many decades and solar cycles, it is now clear that the production of NaK droplets is much more complex than we had previously assumed. Further study is needed to pinpoint which particular parents may be the source of ongoing NaK production. While it was previously believed that atmospheric drag would start to clear this particular population in the near future, we now believe that NaK debris are not likely to be removed from the environment anytime soon, and will continue to contribute to the space debris risk at centimeter debris sizes below 1000 km altitude.

5 REFERENCES

1. Sridharan, R., Beavers, W.I., Gaposchkin, E.M., *et al.* "A Case Study of Debris Characterization by Remote Sensing." MIT Lincoln Laboratory Technical Report 1045 (ESC-TR-97-093), 18 December 1998.
2. Sridharan, R., Beavers, W.I., Gaposchkin, E.M., *et al.* "Radar and Optical Characterization of an Anomalous Orbital Debris Population." *Journal of Spacecraft and Rockets*, 36(5): pp. 719-725, September 1999.
3. Johnson, N.L. *The Soviet Year in Space: 1983*. Teledyne Brown Engineering, Colorado Spring, Colorado, pp. 31-33, 1984.
4. Wiedemann, C., Gamper, E., Horstmann, A., *et al.* "The Contribution of NaK Droplets to the Space Environment." Ed. T. Floher and F. Schmitz, Proc. 7th European Conference on Space Debris (<http://spacedebris2017.sdo.esoc.esa.int>), June 2017.
5. Wiedemann, C., Gamper, E., Horstmann, A., *et al.* "Release of Liquid Metal Droplets from Cosmos 1818 and 1867," IAC-16.A6.2.9. Presented at the 67th International Astronautical Congress, Guadalajara, Mexico, 26-30 September 2016.
6. Xu, Y.-L., Krisko, P.H., Matney, M., *et al.* "Modeling of the Orbital Debris Population of RORSAT Sodium-Potassium Droplets," PEDAS1-0020-10. Presented at the 38th COSPAR assembly, Bremen, Germany, 18-25 July 2010.
7. Nazarenko, A.I., Grinberg, E.I., Nikolaev, V.S., *et al.* "Spacecraft with a Nuclear Power System and Problems of Space Debris." Proc. 4th European Conference on Space Debris (ESA SP-587), August 2005.
8. Foster, J.L., Krisko, P., Matney, M., *et al.* "NaK Droplet Source Modeling." IAC-03-IAA.5.2.02, 2003.
9. Krisko, P.H., and J.L. Foster. "Modeling the sodium potassium droplet interactions with the low earth orbit space debris environment," *Acta Astronautica* 60, pp. 939-945, 2007.